Journal of Experimental Botany, Vol. 59, No. 6, pp. 1149–1161, 2008
doi:10.1093/jxb/ern025
This paper is available online free of all access charges (see http://jxb.oxfordjournals.org/open_access.html for further details)

Journal of Experimental Botany
www.jxb.oxfordjournals.org

RESEARCH PAPER

Expression analysis of *Arabidopsis* vacuolar sorting receptor 3 reveals a putative function in guard cells

Emily L. Avila[1,*], Michelle Brown[1], Songqin Pan[1], Radhika Desikan[2,†], Steven J. Neill[2], Thomas Girke[1], Marci Surpin[1] and Natasha V. Raikhel[1,‡]

[1] *Center for Plant Cell Biology, University of California, Riverside, CA 92521, USA*

[2] *Centre for Research in Plant Science, Genomics Research Institute, University of the West of England, Bristol BS16 1QY, UK*

Received 12 December 2007; Revised 14 January 2008; Accepted 17 January 2008

Abstract

Vacuolar sorting receptors (VSRs) are responsible for the proper targeting of soluble cargo proteins to their destination compartments. The *Arabidopsis* genome encodes seven *VSR*s. In this work, the spatio-temporal expression of one of the members of this gene family, *AtVSR3*, was determined by RT-PCR and promoter::-reporter gene fusions. AtVSR3 was expressed specifically in guard cells. Consequently, a reverse genetics approach was taken to determine the function of *AtVSR3* by using RNA interference (RNAi) technology. Plants expressing little or no *AtVSR3* transcript had a compressed life cycle, bolting ~1 week earlier and senescing up to 2 weeks earlier than the wild-type parent line. While the development and distribution of stomata in *AtVSR3* RNAi plants appeared normal, stomatal function was altered. The guard cells of mutant plants did not close in response to abscisic acid treatment, and the mean leaf temperatures of the RNAi plants were on average 0.8 °C lower than both wild type and another vacuolar sorting receptor mutant, *atvsr1-1*. Furthermore, the loss of AtVSR3 protein caused the accumulation of nitric oxide and hydrogen peroxide, signalling molecules implicated in the regulation of stomatal opening and closing. Finally, proteomics and western blot analyses of cellular proteins isolated from wild-type and *AtVSR3* RNAi leaves showed that phospholipase Dγ, which may play a role in abscisic acid signalling, accumulated to higher levels in *AtVSR3* RNAi guard cells. Thus, AtVSR3 may play an important role in responses to plant stress.

Key words: Abscisic acid, expression analysis, guard cells, hydrogen peroxide, nitric oxide, phospholipase Dγ1, protein trafficking, vacuolar sorting receptor.

Introduction

Soluble proteins are delivered to the vacuole via vesicle trafficking through the endomembrane system. Soluble cargo proteins enter the endomembrane system at the rough endoplasmic reticulum (RER). While some vacuolar proteins segregate into ER bodies that bleb off the ER membrane and are delivered directly to the vacuole (Shimada *et al*., 1997; Tsuru-Furuno *et al*., 2001; Rojo *et al*., 2003), most vacuolar proteins are transported to the Golgi and, subsequently, the trans-Golgi network (TGN) (Vitale and Raikhel, 1999). The TGN represents a major branch point from where soluble proteins enter either the secretory, or default, pathway to the cell's exterior, or are sorted, based on plant-specific primary sequence determinants, and packaged into vesicles for transport to various vacuolar compartments.

Plant cells rely on a diverse array of sequence-specific vacuolar sorting signals (ssVSS) to target cargo proteins

* Present address: Department of Biology, Chaffey College, 5885 Haven Avenue, Rancho Cucamonga, CA 91737-3002, USA.
† Present address: Division of Biology. Imperial College London, South Kensington, London SW7 2AZ, UK.
‡ To whom correspondence should be addressed. E-mail: natasha.raikhel@ucr.edu

Abbreviations: ABA, abscisic acid; BP-80, pea binding protein-80; CCV, clathrin-coated vesicle; ctVSS, carboxy-terminal vacuolar sorting signal; ELP, epidermal growth factor receptor-like protein; ER, endoplasmic reticulum; GUS, β-glucuronidase; NO, nitric oxide; ntVSS, amino-terminal vacuolar sorting signal; PLD, phospholipase D; PSV, protein storage vacuole; RER, rough endoplasmic reticulum; RNAi, interfering RNA; ROS, reactive oxygen species; RT-PCR, reverse transcription PCR; TGN, trans-Golgi network; UCR, University of California, Riverside; UTR, untranslated region; VSR, vacuolar sorting receptor; WT, wild type.

to their proper compartments. The classic model for the plant endomembrane system has been that carboxy-terminal vacuolar sorting signals (ctVSS) have been found necessary for correct targeting of tobacco barley lectin (Bednarek *et al*., 1990), tobacco chitinase A (Neuhaus *et al*., 1991), and β-1, 3-glucanase (Melchers *et al*., 1993) to the protein storage vacuole (PSV), and amino-terminal vacuolar sorting signals (ntVSS) direct proteins such as barley aleurain (Holwerda *et al*., 1992) and sweet potato sporamin (Matsuoka and Nakamura, 1991) to the lytic vacuole. Proteins such as phytohaemagglutinin (Tague *et al*., 1990) and legumin (Saalbach *et al*., 1991) contain internal sorting signals that are not cleaved and, in addition, there is evidence that some proteins are sorted based on information provided by multidomain signals (Saalbach *et al*., 1991). There appears to be a correlation between the type of VSS and the pathway taken to the destination compartment. Proteins containing ctVSS are packaged into dense vesicles (Matsuoka *et al*., 1995; Hohl *et al*., 1996), and are delivered to PSVs (Hohl *et al*., 1996; Paris *et al*., 1996). ntVSS-containing proteins are transported to the lytic vacuole by clathrin-coated vesicles (CCVs) in a pathway that appears to be analogous to those described for yeast and mammalian cells (Ahmed *et al*., 2000). It was recently proposed that different types of vacuoles may not co-exist in single cells, but that the post-embryonic PSV matures into a lytic vacuole (Olbrich *et al*., 2007). The ntVSS has been characterized in several plant species and was often found to contain an NPIR motif (Matsuoka and Nakamura, 1999), although this conservation is not absolute. The NPIR motif is recognized by vacuolar sorting receptors (VSRs), among these are pea binding protein-80 (BP-80) (Kirsch *et al*., 1994), pumpkin PV72 (Shimada *et al*., 2002), and *Arabidopsis thaliana* VSR1/ELP (vacuolar sorting receptor 1/epidermal growth factor receptor-like protein) (Ahmed *et al*., 1997). Pea BP-80 was isolated using affinity chromatography of CCVs to identify proteins that bind the ntVSS of barley aleurain (Kirsch *et al*., 1994). PV72 was isolated from precursor-accumulating vesicles of developing pumpkin seeds (Shimada *et al*., 1997). *Arabidopsis* VSR1/ELP was identified, using a bioinformatics approach, to find proteins that contained cysteine-rich repeats that are present in the receptor proteins of other species (Ahmed *et al*., 1997).

Plant VSR domain structure is highly conserved. VSRs are type I transmembrane proteins with large lumenal domains, short transmembrane domains, and small cytoplasmic domains (Ahmed *et al*., 1997). The immature forms of these proteins contain an amino-terminal signal peptide necessary for co-translational insertion into the ER membrane (Ahmed *et al*., 1997). A protease-associated domain, the proposed site of ligand interactions, follows the signal peptide (Mahon and Bateman, 2000). There are three cysteine-rich epidermal growth factor repeats within the lumenal domain, one of which is a calcium-dependent epidermal growth factor repeat (Watanabe *et al*., 2002). The cytoplasmic domain features a tyrosine motif that interacts with clathrin coat adaptor proteins at the TGN (Sanderfoot *et al*., 1998; Bonifacino and Dell'Angelica, 1999; Watanabe *et al*., 2002; Happel *et al*., 2004). It also contains a diacidic motif that directs export from the ER (Matsuoka and Bednarek, 1998).

AtVSR1 and BP-80 have been localized to the TGN, CCVs, and the PVC, and colocalize with proteins such as aleurain and sporamin that are destined for the lytic vacuole (Kirsch *et al*., 1994; Ahmed *et al*., 1997, 2000; Sanderfoot *et al*., 1998; Li *et al*., 2002). These locations are consistent with those for MPR and Vps10, vacuolar/lysosomal sorting receptors of animals and yeast. Both sorting receptor proteins have also been found to co-localize with the plant syntaxin SYP21 (Miller *et al*., 1999; Ahmed *et al*., 2000).

The current model of plant VSR function in the context of the CCV pathway is as follows: the NPIR motif of the ntVSS interacts with the ligand-binding domain of the VSR in the neutral pH lumen of the TGN, the cytoplasmic domain of the VSR is recognized by the trafficking machinery and, subsequently, both proteins are packaged into CCVs that are then delivered to the PVC (Ahmed *et al*., 2000). The receptor releases the cargo in the acidic pH environment of the PVC and is presumably recycled to the TGN by vesicle trafficking, whereas the cargo is delivered to the lytic vacuole by either vesicle trafficking or fusion of the PVC with the vacuole.

Two observations suggest a more complicated scenario. First, the *Arabidopsis* genome encodes six additional genes that are highly similar to AtVSR1/AtELP and thus, may also function as VSRs (Laval *et al*., 1999; Shimada *et al*., 2003; Masclaux *et al*., 2005). Additionally, rice encodes nine genes that are homologous to AtVSR1/AtELP and BP-80 (E Avila, T Girke, and N Raikhel, unpublished results). Secondly, despite their high amino acid identity, plant VSRs are found in a variety of vesicle types and these have been implicated in different vacuolar transport pathways. A recent reverse genetics characterization of the *Arabidopsis* VSRs demonstrated that VSR1 could mediate the transport of 2S albumin, a seed storage protein, to PSVs in developing seed (Shimada *et al*., 2003). Furthermore, the putative receptor for *Vigna mungo* SH-EP, a KDEL-tailed cysteine protease that degrades storage proteins in the PSV, was found to be homologous to AtVSR1 (Tsuru-Furuno *et al*., 2001). These results were further reinforced by the examination of transport of storage proteins, their cognate processing proteases, and the VSR1 protein during PSV formation in *Arabidopsis* embryos. Storage proteins and their corresponding processing proteases were spatially separated in the Golgi cisternae and subsequently packaged into separate vesicles. In this study, only vesicles that

contained the storage proteins were marked by VSR1. Subsequently, both the storage protein vesicles and processing protease vesicles fused into a prevacuolar multivesicular body (Otegui *et al*., 2006).

However, previous results demonstrated that AtELP/VSR1 mediates the transport of ntVSS, and not ctVSS-containing proteins (Ahmed *et al*., 2000). A more recent study, in which the distribution of two VSRs and two types of luminal cargo proteins was examined, showed that cruciferin, a storage protein, and aleurain, a processing protease, were both transported to the PSV during the bent-cotyledon stage of *Arabidopsis* embryo development. Also examined were the localizations of the sorting receptors VSR1 and RMR, which may be the sorting receptors of aleurain and cruciferin, respectively. RMR, which recognizes ctVSSs, had a distribution similar to that of cruciferin and was found in dense vesicles, and therefore are the more likely candidates for sorting storage proteins. VSR1 was localized primarily to the TGN. The authors hypothesized that, although there was spatial separation between the receptors and ligands, their pathways are interdependent; therefore a lesion in one could influence the function of the other (Hinz *et al*., 2007).

In order to develop a more comprehensive model of VSR function in plants, the expression patterns of one of the *Arabidopsis VSR* genes was determined, *AtVSR3*, using both reverse transcription PCR (RT-PCR) and stably transformed promoter::GUS (β-glucuronidase) fusion lines. In addition, the phenotype of plants that post-transcriptionally silenced the *AtVSR3* gene was characterized, and it was determined that AtVSR3 may mediate abscisic acid (ABA)-related responses in guard cells.

Materials and methods

Plant growth conditions

Arabidopsis seeds (ecotype Columbia) were sterilized in a solution of 50% bleach/0.05% Tween-20 (Sigma) and rinsed with sterile water. After cold treatment at 4 °C for 24 h, the seeds were sown on phytagar plates containing Murashige Minimal Organics Medium (Invitrogen/Gibco), and antibiotic selection as indicated. The seedlings were germinated under constant light conditions at ~ 23 °C. After 2 weeks, the seedlings were transferred to a commercial soil mixture containing slow-release fertilizer pellets (Osmocote) and fungicide (Marathon). The plants were grown under long-day conditions (16 h light/8 h dark) at ~23 °C. For experiments carried out under short-day conditions, the plants were grown in a chamber set at 8 h light, 16 h dark, at ~23 °C.

Phylogenetic analysis and bioinformatics

The phylogenetic tree was calculated with the PHYLIP package (Felsenstein, 1997) using the PROTDIST program for calculating the distance matrix (categories model as distance matrix), the Neighbor–Joining method for tree construction, and the midpoint method in RETREE for defining the root of the tree. The internal bootstrap values were obtained from 100 alignment re-sampling replicates. Related protein sequences were identified by BLASTP searches against the protein sequences from *Arabidopsis* (TAIR annotation 7), rice (TIGR annotation 5), and the UNIPROT database using an E value of $1e^{-20}$ as cut-off. The sequences obtained were aligned with the T-Coffee program (Notredame *et al*., 2000).

RT-PCR of AtVSR3

Gene-specific primers were designed for *VSR3* and were synthesized at the MSU Macromolecular Structural Facility. The forward primer sequence was CCT TGT CCT TCG AAT TTG TTC TTT G and the reverse primer TCT AGA GTC CTT CCC GGG GAA TAA ATA GAT G. Total RNA was extracted from all tissues using the RNeasy Kit (Qiagen). RT-PCR was carried out using the One-Step RT-PCR Kit (Qiagen) with 500 ng total RNA template. Each PCR reaction was limited to 28 cycles in order to stay within the linear range of amplification and thus obtain a more accurate picture of the relative levels of gene expression in the various tissues. The PCR products were electrophoresed on 1% agarose gels stained with ethidium bromide and photographed using a Bio-Rad gel documentation system. All the PCR products were sequenced at the University of California, Riverside (UCR) Center for Genomics DNA Sequencing Core Facility.

Preparation of the VSR3 *promoter::GFP:GUS construct*

The pRJG23 construct was a generous gift from Dr Jen Sheen. For ease of cloning into pCAMBIA, the GFP::GUS fragment of pRJG23 was cloned into pBS (SK^+) using an *Eco*RI/*Hin*dIII double digest. The GFP::GUS fragment was then cloned into pCAMBIA 1300MCS by means of a *Kpn*I/*Sac*I double digest. The subsequent ligation yielded pCAMBIA::GFP:GUS.

The 2160 bp region upstream of the *AtVSR3* start codon was amplified by PCR using the following primers: forward ATA AGC TTA ACG ACT ACT GCG TAT TGG AGA GC; reverse ATA AGC TTT GGA AGG TAA CAC AGA AGC TGC. *Hin*dIII restriction enzyme sites (underlined) were added to facilitate cloning. The promoter was amplified from wild-type (WT) Columbia genomic DNA using Takara Ex-Taq DNA polymerase and following the manufacturer's protocol. The PCR products were purified using Qiagen PCR purification columns and were subsequently cloned into the pGEM-T Easy vector (Promega). Sequencing of the PCR products and the constructs was carried out at the UCR DNA Sequencing Core Facility.

To replace the *35S* promoter with the *VSR3* promoter, *35S::GFP:GUS* and *pGEM::VSR3p* were digested with *Hin*dIII, and purified using Quiagen columns. The vector was treated with alkaline phosphatase and ligated with T4 DNA ligase.

The resultant construct was cloned into the pCAMBIA1300 binary vector (McElroy *et al*., 1995) and transformed into WT *Arabidopsis* (Columbia ecotype) by *Agrobacterium*-mediated stable transformation (Clough and Bent, 1998). Seeds were collected from the transformed plants and germinated on agar containing Murashige Minimal Organics Medium, 30 mg l^{-1} hygromycin (Sigma), and 25 mg l^{-1} Carbenecillin (Sigma).

Plant transformation

The DNA constructs were transformed into *Agrobacterium tumefaciens* via a freeze–thaw protocol (Sanderfoot *et al*., 2001). Transformed agrobacteria were selected on the appropriate media at 28 °C, and antibiotic-resistant colonies were screened for the presence of the construct using PCR and by restriction digests of isolated DNA. The constructs were introduced into *Arabidopsis* via *Agrobacterium*-mediated transformation using the floral dip method (Clough and Bent, 1998), and the putative transformants were selected for resistance to hygromycin. The T_2 and T_3 generations were then tested for GUS activity.

Photography and microscopy

Seedlings were examined and photographed with a Leica MZIII dissection microscope equipped with a Canon G4 digital camera. Microscopy of guard cells was carried out using a Meridian insight confocal microscope fitted with ×20 and ×40 objectives. Micrographs were taken with a Hammamatsu CCD camera.

Nucleic acid extraction from plants and subsequent analysis

Genomic DNA was extracted from rosette leaves of individual plants following published protocols (Weigel and Glazebrook, 2002). PCR was carried out using Ex-Taq (Takara Shuzo) and following the manufacturer's instructions. Total RNA was extracted from rosette leaves using the RNeasy Plant Mini Kit (Qiagen). RT-PCR was carried out using 500 ng total RNA, unless otherwise indicated, with the One-Step RT-PCR Kit (Qiagen) following the manufacturer's protocol.

Post-transcriptional silencing of the AtVSR3 *gene*

The pFGC5941 dsRNA vector was a generous gift from Dr Richard Jorgensen and Dr Vicki Chandler, and the relevant DNA fragments were inserted following the protocols outlined on the ChromDB web page (http://ag.arizona.edu/chromatin/strategy.html). Primers were designed to amplify the coding region for the last 10 amino acids of the carboxy-terminal and the 3′ untranslated region (UTR) of *AtVSR3*: forward TCT AGA GGC GCG CCT CCC GAA CCA CGT TGA ATG ATG AAC G; reverse GGA TCC ATT TAA ATA ACA ACA TGA ACT CTA AAA CAA GTA AC. The forward primer contained *Xba*I and *Asc*I restriction enzyme sites (underlined) for cloning purposes. The reverse primer added *Bam*HI and *Swa*I restriction sites (underlined) to the 3′ end, also for cloning purposes. The PCR product was cloned into pGEM-T Easy (Promega) and sequenced at the UCR DNA Sequencing Facility. To add the 3′ end of *AtVSR3* in the forward orientation, the construct and the vector were digested with *Asc*I and *Swa*I. The relevant digestion products were resolved on a 1% low melt agarose gel and the DNA purified from the gel using Qiagen columns. The products were ligated with T4 DNA Ligase (Roche) and transformed into *Escherichia coli* DH5α. To add the same *AtVSR3* fragment in the opposite orientation, the new construct and the pGEM construct were digested with *Bam*HI and *Xba*I, ligated, and transformed as described above. The integrity of the final construct was confirmed by triple restriction digest with *Not*I, *Eco*RI, and *Pst*I. The construct was transformed into *Arabidopsis* using the same protocols outlined above. Transgenic seedlings were obtained by germinating the seeds on selection media. RT-PCR was carried out for all putative transformants using the *AtVSR3* RT-PCR primers.

Stomatal bioassays

Leaves were floated in MES/KCl buffer (5 mM KCl/10 mM MES/50 μM $CaCl_2$, pH 6.15) for 3 h under continuous illumination (60–100 μE m^{-2} s^{-1}). Once the stomata were fully open, leaves were treated with ABA for a further 2.5 h. The leaves were subsequently individually homogenized in a Waring blender for 30 s and the epidermal fragments collected on a 100 μm nylon mesh (SpectraMesh, BDH-Merck, UK). Stomatal apertures from epidermal fragments were then measured using a calibrated light microscope attached to an imaging system (Leica QWin software, Leica, UK).

Measurement of hydrogen peroxide (H_2O_2) and nitric oxide (NO) using confocal microscopy

Epidermal fragments from mature leaves, prepared as described above, were incubated in MES/KCl buffer for 2–3 h. Following buffer treatment, the fragments were loaded by incubation in 50 μM of the H_2O_2-sensitive fluorescent dye H_2DCFDA (Molecular Probes, Leiden, The Netherlands) or 15 μM DAF2-DA (Calbiochem, UK) for 10 min. After washing in fresh buffer for a further 20 min, the fragments were challenged with ABA. Controls included the addition of the appropriate solvents. Confocal laser scanning microscopy was used to visualize fluorescence, using an excitation wavelength of 488 nm and an emission wavelength of 515–560 nm (Nikon PCM2000; Nikon Europe B.V. Badhoewvedorp, The Netherlands). Images were acquired and analysed using Scion Image software (Scion Corp., Frederick, MD, USA) to measure the relative fluorescence intensities in the cells following various treatments. Data represent fluorescence intensities from several guard cells analysed in different experiments.

Thermal analysis of seedlings

Seedlings were grown as described for the germination assay for 2 weeks without ABA. The plates were photographed with a retail-grade digital camera and analysed with a ThermaCAM 560 from FLIR Systems (Boston, MA, USA).

Proteomic analysis

Total proteins were extracted from either WT or VSR3 interfering RNA (RNAi) guard cells that were isolated using published protocols (Pandey *et al*., 2002). The proteins were separated by standard 18 cm 14% SDS–PAGE (Laemmli, 1970). Staining with Coomassie Brilliant Blue R 250 showed a ~90 kDa protein band with differences in staining intensity between WT and *VSR3* RNAi guard cells. This band was excised and subjected to LC/MS/MS analysis to identify the constituent proteins. Briefly, the two gel slices were cut into small pieces ~1 mm^2 in size, destained, and then digested overnight with trypsin at 37 °C. The tryptic peptides were extracted following a procedure described previously (Pan *et al*., 2003). The liquid chromatography (LC) configuration and method, the mass spectrometer instrumentation parameters, and the data-dependent analysis survey scanning method were the same as described (Carter *et al*., 2004). The data-dependent analysis data were then processed with the PLGS2 program (Waters, Milford, MA, USA) to generate PKL text files that were submitted to MASCOT database searching to identify proteins with the same parameters as previously described (Carter *et al*., 2004). The mass spectrometer used in this study was a Q-TOF AP US (Waters) housed in the W.M. Keck Proteomics Laboratory at the Center for Plant Cell Biology.

For the phospholipase Dγ (PLDγ) western blot, leaves were excised from WT and *VSR3* RNAi plants. Equal amounts of tissue were used to make crude extracts. The tissues were broken in 100 μl Laemmli buffer (Laemmli, 1970) and centrifuged for 1 min at 1000 *g*. The supernatants were then heated to 100 °C for 5 min. Fifty microlitres of each extract were loaded onto a 10% SDS–PAGE gel. The transfer and western blot were carried out using standard protocols (Sambrook and Russell, 2001). The blot was incubated with a 1:2000 dilution of PLDγ antibody, kindly provided by Dr Xuemin Wang (Donald Danforth Plant Science Center).

Results

Phylogenetic analysis and expression patterns of the AtVSR *gene family*

Based on the analyses shown in Fig. 1 and published phylogenetic analyses (Shimada *et al*., 2003; Masclaux *et al*., 2005), the known plant VSRs clustered into three

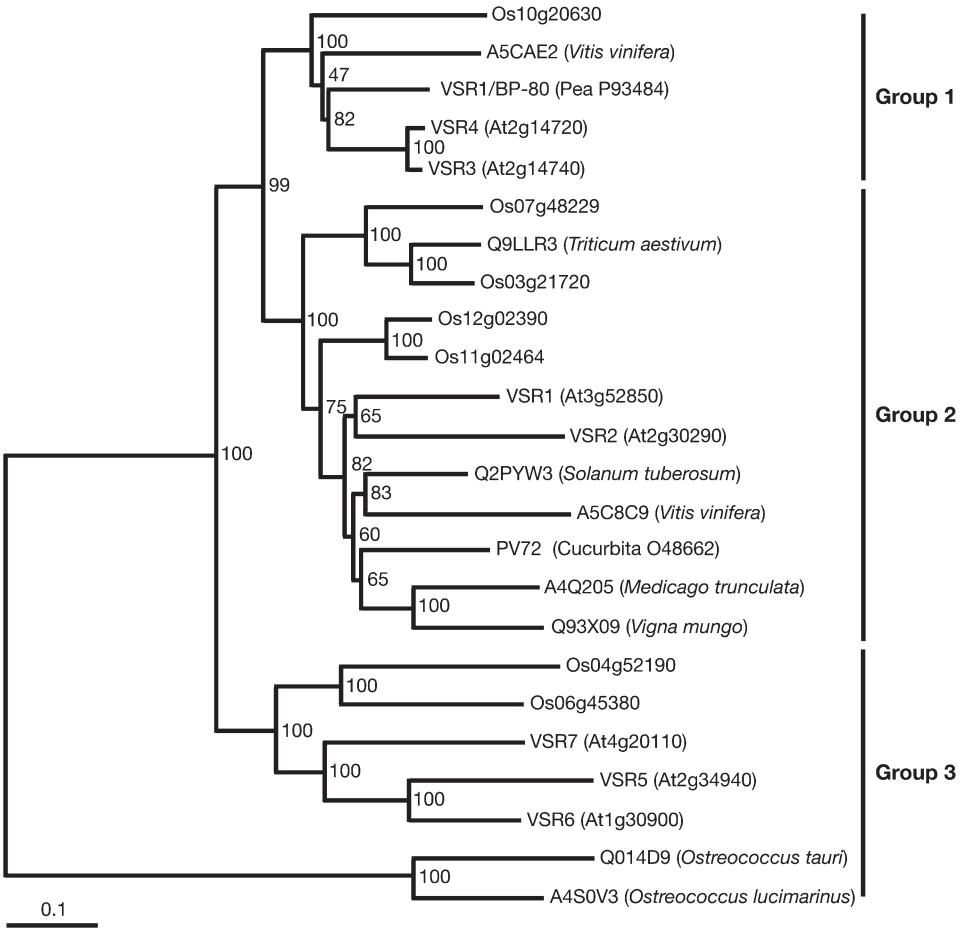

Fig. 1. Phylogenetic analysis of plant VSRs. Phylogenetic analysis indicated that the land plant clade of the vacuolar sorting receptor proteins clusters into three groups. The full-length amino acid sequences were analysed to determine their relationships to one another. The bootstrap values are reported at the nodes.

groups. The first group contained *Arabidopsis* VSRs 3 and 4, pea BP-80, a grape (*Vitus vinifera*) VSR, and a rice VSR. The second group was composed of AtVSR1, AtVSR2, pumpkin (*Cucurbita*) PV-72, four rice VSRs, and one VSR each from wheat (*Triticum aestivum*), potato (*Solanum tuberosa*), grape, mung bean (*Vigna mungo*), and *Medicago trunculata*. The third group contained VSRs 5–7, two rice VSRs, and VSRs from two different species of green algae.

All the putative plant VSRs contain a proteinase-associated domain, thought to be the site of cargo loading (Mahon and Bateman, 2000). The phylogenetic relationship of the proteinase-associated domains was examined and found to be identical to that of the full-length proteins (data not shown), suggesting that the relatedness of the individual proteins may be indicative of their functions. To begin to address the particular functions of individual *Arabidopsis* VSRs, the expression patterns of the *AtVSR3* gene were determined using RT-PCR.

RT-PCR was carried out using gene-specific primers to amplify total RNA isolated from various *Arabidopsis* tissues. The primers were specific to the 5′ and 3′ UTRs of the *VSR3* gene, and amplified a 1.9 kb product that was specific for the cDNA. After reverse transcription, PCR was carried out for a total of 28 cycles. *AtVSR3* transcripts were detected in all tissues, with the exception of seeds,

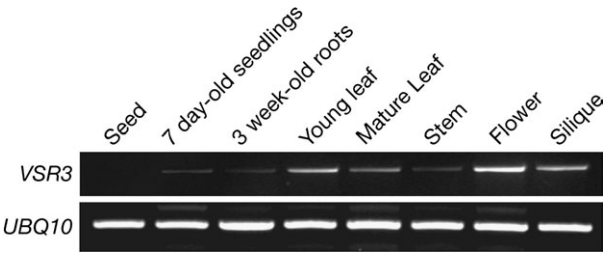

Fig. 2. Expression analysis of the *Arabidopsis VSR3* gene. RNA was extracted from various *Arabidopsis* tissues as indicated in the figure. Five hundred nanograms of RNA were used as a template for RT-PCR with gene-specific primers and 28 cycles of PCR after reverse transcription cDNA synthesis. The *Arabidopsis UBIQUITIN10* gene was used as a control.

although expression was highest in young leaves, flowers, and siliques (Fig. 2).

Cell type-specific expression patterns of Arabidopsis *VSRs*

To determine the cell type-specific expression patterns of AtVSR3, the predicted promoter region of the *VSR3* gene was fused to the coding region of the β-glucuronidase (GUS) reporter gene. The transcriptional fusion was transferred to a binary vector for stable transformation into *Arabidopsis*. Fifteen transgenic lines from three independent pools of plants carrying the *pAtVSR3*::GUS reporter construct were analysed. In a departure from the RT-PCR results, faint GUS staining was detected in the cotyledons of imbibed seeds (Fig. 3A). The staining was considerably fainter than that in other tissues; most likely increasing the number of RT-PCR cycles would have revealed the presence of *VSR3* transcript. Thus, if *VSR3* is expressed in *Arabidopsis* embryonic tissue, it is at very low levels. GUS activities in other tissues at various developmental stages essentially mirrored the RT-PCR results. GUS activity was observed throughout 7-d-old seedlings (Fig. 3B). In older plants, GUS staining was detected in 3-week-old roots (Fig. 3C). GUS staining in young leaves was concentrated in the vascular tissue and was uniform over the rest of the leaves (Fig. 3D). However, as the seedlings matured, expression from the *AtVSR3* promoter was strongest in vascular tissue, guard cells, and hydathodes of true leaves (Fig. 3E, F). GUS activity was also detected in the inflorescence stems, flowers, and siliques (Fig. 3G–J). In siliques, GUS staining was found primarily in the siliques sheaths and funiculi (Fig. 3I, J).

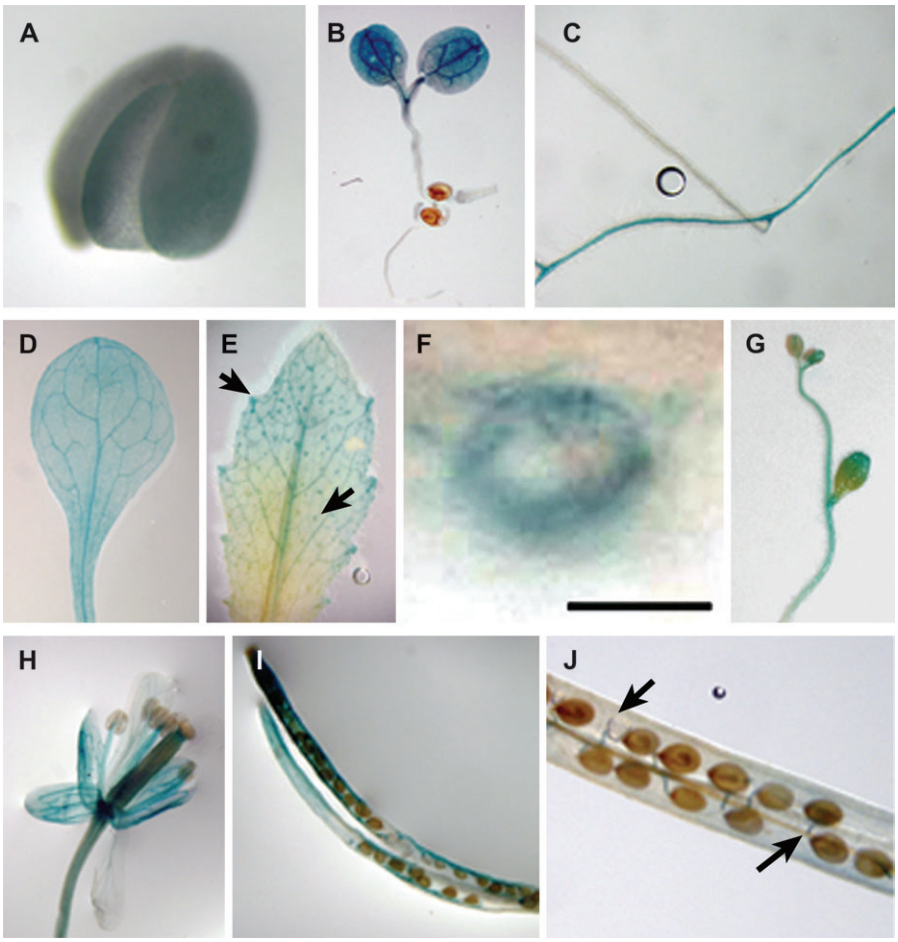

Fig. 3. Expression analysis of the *Arabidopsis* VSR3 protein using promoter::GUS fusions. AtVSR3 promoter::GUS transgenic plants were histochemically stained with the X-glucuronide substrate so as to visualize its tissue and cell type-specific expression patterns. The images presented are typical examples of staining as observed from multiple independent lines. (A) GUS activity is seen in the mature embryo. (B) Seven-day-old seedlings express GUS throughout the cotyledons, hypocotyl, and vascular tissue. (C) GUS is detected in 3-week-old roots. (D) Staining of the adaxial surface of a young leaf. (E) A view of the abaxial surface of a mature leaf. Arrows point to a stained hydathode and stomate. (F) Close examination of rosette leaves (×40 magnification) revealed GUS activity specifically in the guard cells. Scale bar=20 μm. (G) GUS activity was detected in the inflorescence stem. (H) Staining of carpel, anthers, and petals in *pVSR3::GUS* flowers. (I) GUS activity detected in the silique sheaths. (J) Within the siliques, GUS staining was restricted to the funiculi (arrows).

Creation of RNAi lines for functional analysis of AtVSR3

Promoter::reporter fusion studies indicated that *AtVSR3* was expressed in guard cells, thus suggesting that the VSR3 protein may play a role in stomatal function. Thus, a reverse genetics approach was taken to determine the function of *AtVSR3*. It was not possible to obtain viable, homozygous T-DNA knockouts for *AtVSR3* (data not shown), indicating that this was an essential gene, so the function of *AtVSR3* was addressed by creating RNAi lines that post-transcriptionally reduced the accumulation of *AtVSR3* transcript. RNA was extracted from putative RNAi lines and used as templates for semi-quantitative RT-PCR. Four of the transformed lines, Lines 1.11, 1.18, 2.6, and 3.1, which were generated in three independent transformations, showed greatly reduced levels of *AtVSR3* transcript (Fig. 4A).

AtVSR3 *RNAi plants have a compressed life cycle*

Comparison of the four *AtVSR3* RNAi plant lines with WT plants indicated that the RNAi lines had a compressed life cycle relative to WT (Fig. 4B, C). Seeds from all four lines were germinated on soil under short-day light conditions. While all the RNAi lines and the WT reference bolted at approximately the same number of leaves (Fig. 4B), the RNAi lines bolted around 7–10 d earlier than WT. Furthermore, the *AtVSR3* RNAi plants set seed and senesced about 2 weeks earlier than WT plants when grown under the same environmental conditions (data not shown). Similar effects were observed in RNAi plants that were grown under long-day conditions, except that bolting occurred 5–7 d earlier than in WT (Fig. 4C and data not shown).

Loss of AtVSR3 protein results in altered stomatal function

Because of the guard cell expression patterns that were observed for *AtVSR3*, it was questioned whether the *AtVSR3* RNAi plants exhibited an abnormal distribution or function of guard cells. Analysis of rosette leaves from various stages of development showed that the RNAi lines had essentially the same numbers of stomates as their WT counterpart, indicating that the loss of AtVSR3 protein does not affect stomatal number or distribution (data not shown). However, when measuring whether cells are opened or closed based on a 2.5 μm cut-off, there are

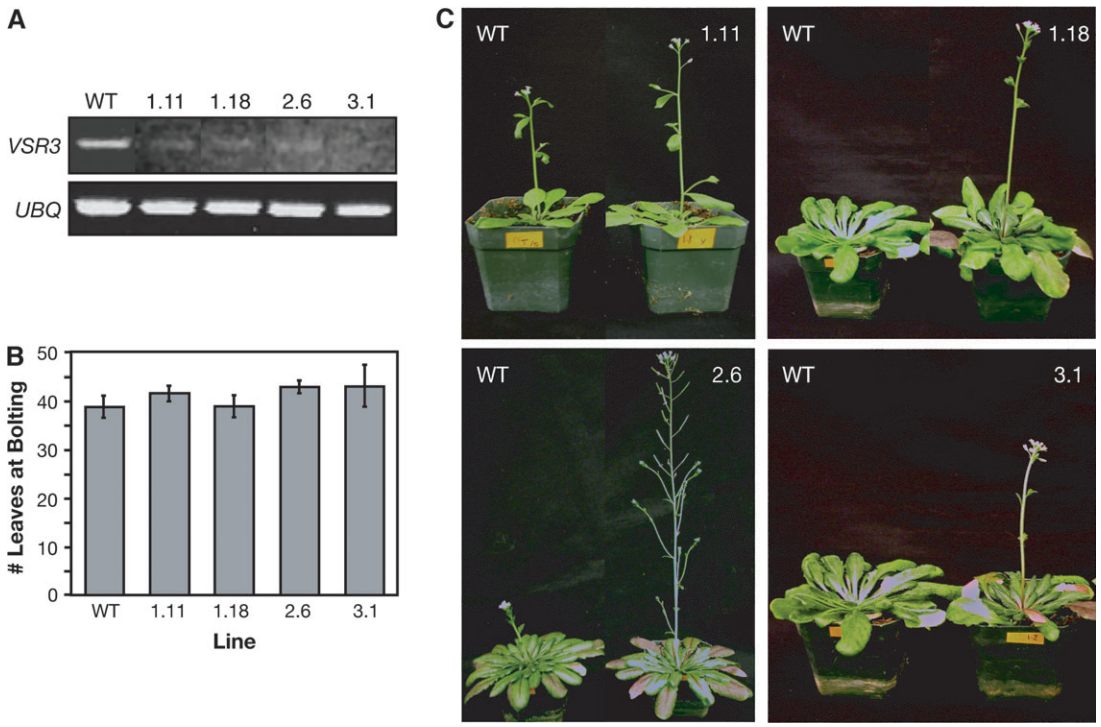

Fig. 4. Characterization of *AtVSR3* RNAi plants. (A) RT-PCR of wild-type (WT) and four putative transformants using either *AtVSR3*-specific primers (top panel) or *UBIQUITIN10*-specific primers (bottom panel). While some transformants had reduced amounts of *AtVSR3* mRNA, one line, Line 3.1, did not accumulate any detectable AtVSR3 mRNA, while *UBIQUITIN10* levels for all lines examined were similar. (B, C) *AtVSR3* RNAi plants have a shorter life cycle than WT plants. Plants were grown in a short-day chamber. WT and *AtVSR3* RNAi plants have the same number of leaves at bolting (B). (C) *AtVSR3* RNAi plant growth compared with WT. The *AtVSR3* RNAi plants from Lines 1.11, 1.18, 2.6, and 3.1 (right) are considerably larger and more developed than their WT counterparts. Line 1.11 and its WT comparison were grown under long-day conditions and are 30 d old. Lines 1.18 and 3.1 were grown under short-day conditions and are 56 d old. Line 2.6 was also grown under short-day conditions and is 61 d old.

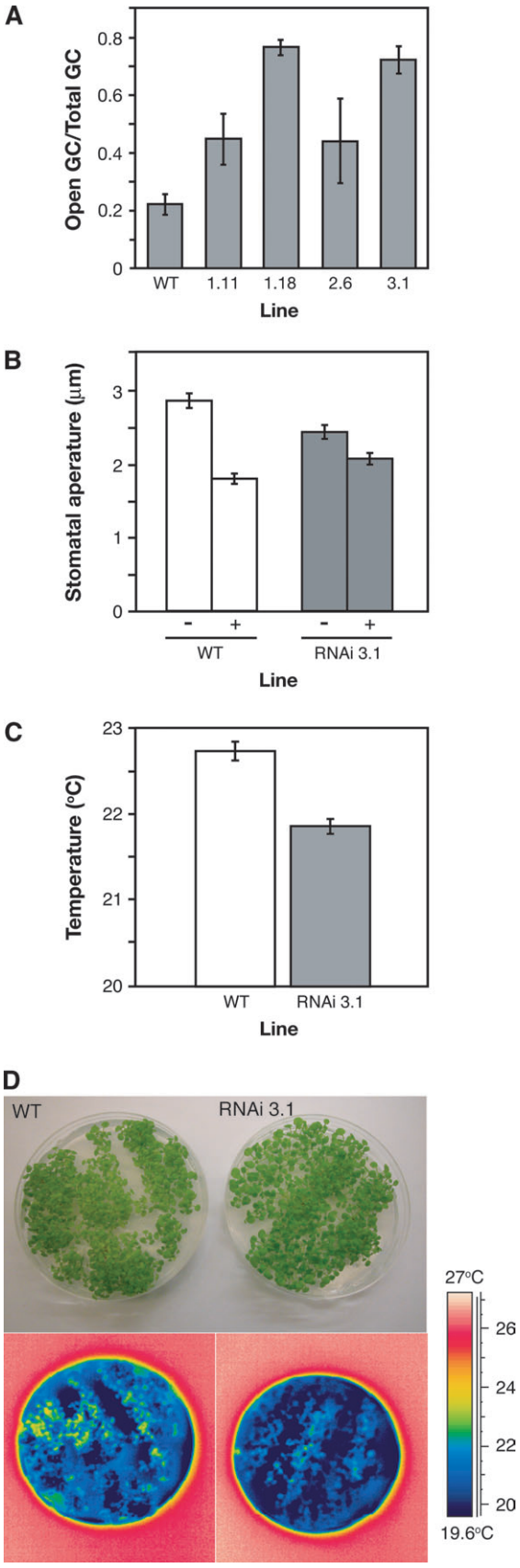

significant differences between the WT and the RNAi lines (Fig. 5A).

Because Line 3.1 did not accumulate any detectable *AtVSR3* transcript, this line was used for all subsequent experiments. In a more detailed analysis of Line 3.1, the stomatal apertures in WT and mutant lines were measured with and without treatment with ABA. As shown in Fig. 5B, in the absence of ABA the apertures of *AtVSR3* RNAi were smaller than WT; however, with ABA, there was only a very small closure response in the mutant compared with the WT.

If stomata of the mutants did not fully close in response to ABA, then the plants would have higher rates of transpiration, and thus the leaves would display cooler temperatures than leaves of WT plants (Merlot *et al*., 2002). Furthermore, if AtVSR3 specifically functioned in stomatal regulation, then plants with defects in other members of the AtVSR family would most likely have leaf temperatures similar to that of WT. Thus, a thermal camera was used to compare the temperatures of WT leaves with the leaves of both *AtVSR3* RNAi plants (Line 3.1) and *vsr1-1* mutant plants (Fig. 4C, D, and data not shown) (Shimada *et al*., 2003). The analysis demonstrated that the mutants were on average 0.8 °C (P <0.0001) cooler than both their WT counterparts and the *atvsr1* mutant (Fig. 5C and data not shown). These results indicated that AtVSR3 plays a role in guard cell movement and that its function is not redundant with at least one other member of the AtVSR family.

Loss of AtVSR3 results in altered accumulation of NO and H_2O_2

NO and H_2O_2 have been implicated in regulation of stomatal opening and closing. Furthermore, the levels of NO and H_2O_2 increase in the presence of ABA in WT plants (Pei *et al*., 2000; Desikan *et al*., 2002). Therefore, the amounts of NO and H_2O_2 were compared in WT and AtVSR3 RNAi Line 3.1 plants, both untreated and treated with ABA. The levels of both signalling molecules were

Fig. 5. Stomatal function is impaired in the *AtVSR3* RNAi lines. (A) Examination of the stomata of excised leaves at high magnification revealed that *AtVSR3* RNAi lines did not have as many closed stomata as their wild-type counterparts under the same conditions. Closed stomata were considered to be those that had a diameter <2.5 μm. (B) ABA-induced stomatal closure. Leaves from either wild-type (WT) or the *AtVSR3* RNAi Line 3.1 were incubated in buffer alone (–) or in 10 μM ABA (+). Data are from three independent experiments (mean ±SE; n=60 guard cells). (C, D) Thermal imaging of WT and *AtVSR3* RNAi Line 3.1 plants. Seeds were sown on agar plates and grown for 2 weeks (D, top; wild type on left and *AtVSR3* RNAi Line 3.1 on right). The plates were imaged with a thermal camera (D, bottom; wild type on left and *AtVSR3* RNAi on right) and the results are presented in a colour format with a corresponding look-up table. The temperatures of random spots on the plate were collected and compared between the wild-type and mutant plates (D). The average temperature was 0.8 °C higher in wild-type plants with a significance of P <0.0001.

constitutively higher in untreated *AtVSR3* RNAi plants, compared with untreated WT plants (Fig. 6). Treatment of WT plants with ABA raised H_2O_2 and NO levels nearly 2-fold, compared with the untreated WT plants (Fig. 5). H_2O_2 and NO levels were actually reduced by small but significant amounts in treated versus untreated *VSR3* RNAi Line 3.1 plants, by 12% and 13%, respectively. Because both H_2O_2 and NO levels are already elevated in untreated RNAi plants, this decrease may reflect a negative feedback regulatory pathway (Desikan *et al*., 2004).

Comparison of accumulated proteins in WT and RNAi AtVSR3 *plants*

The next goal was to determine the molecular relationship between AtVSR3, endomembrane trafficking, and stomatal movement. Toward this end, total proteins were isolated from WT and *AtVSR3* RNAi guard cell protoplasts. The isolated proteins were separated by SDS–PAGE and visualized by Coomassie stain. There were differences in protein composition observed between the WT and *AtVSR3* RNAi extracts (data not shown). A protein band of ~90 kDa that stained more heavily in the RNAi line than the WT was identified using LC-MS. The sole endomembrane system protein in the 90 kDa band that had different accumulation patterns in WT and *AtVSR3* RNAi was phospholipase Dγ1 (PLDγ1; At4g11850). PLDγ is present in a number of different plant tissues, and participates in a variety of cellular processes; amongst these are vesicular trafficking and signal transduction pathways (Zhang *et al*., 2005). To confirm the difference in accumulation patterns of PLDγ between WT and *AtVSR3* RNAi plants, antibodies against PLDγ were used in a western blot comparison of crude protein extract from leaves of WT and *AtVSR3* RNAi Line 3.1 (Fig. 7). The PLDγ protein accumulated more in the RNAi plants than in the WT or other mutant plants such as *vsr1-1* (data not shown). Quantification of the blot using the ImageJ analysis package showed that mutant plants contained 2.75-fold more protein than WT plants. This result indicates that there may be a functional relationship between AtVSR3 and PLDγ.

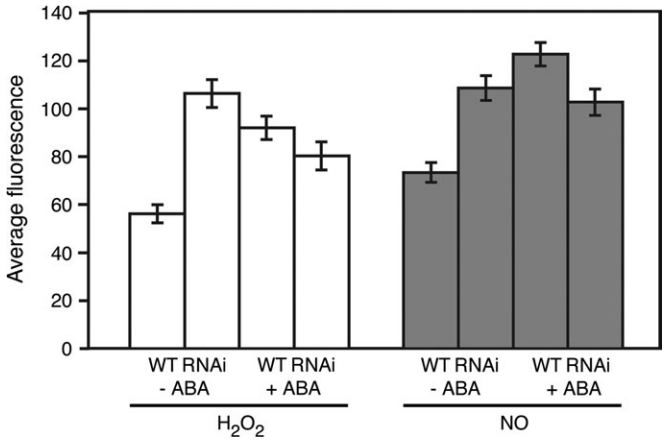

Fig. 6. Generation of H_2O_2 and NO in response to ABA. Epidermal fragments from either WT or *AtVSR3* RNAi Line 3.1 leaves exposed to either buffer alone (–) or 10 μM ABA (+) for 15 min (H_2O_2) or 30 min (NO) were subjected to confocal microscopy and detection of H_2O_2 or NO fluorescence. Data are represented as average pixel intensities (mean ±SE) recorded from 85–130 guard cells. White columns indicate H_2O_2 levels; grey columns indicate NO levels.

Discussion

Phylogenetic studies and expression analysis of Arabidopsis *VSRs suggest possible functions for individual family members*

Little is known about the functions of the individual members of the *Arabidopsis* family of VSRs, with the possible exception of AtVSR1. Formerly referred to as AtELP, it has been shown to bind the ntVSSs of barley aleurain and sporamin (Ahmed *et al*., 2000), and also the ctVSS of *Arabidopsis* 12S globulin in a Ca^{2+}-dependent manner (Shimada *et al*., 2003). Studies with VSR1 knockout lines demonstrated that *atvsr1-1* and *atvsr1-2* accumulated the precursors of two seed storage proteins, suggesting that this receptor mediates transport to the PSVs of developing seeds (Shimada *et al*., 2003; Otegui *et al*., 2006). However, more recent data call this hypothesis into question (Hinz *et al*., 2007); it may be more accurate to state that this group of VSRs is important for the process of sorting to the PSV, but they themselves are not the actual sorting receptors for storage proteins.

The second group of VSRs was composed of the previously characterized pea BP-80, two homologues from *Arabidopsis*, AtVSR3 and AtVSR4, and putative VSRs from rice and grape. BP-80 was identified as a VSR for the CCV pathway and is strictly localized to CCVs relative to dense vesicles (Kirsch *et al*., 1994). Thus, members of this group may be responsible for soluble proteins that are delivered to the lytic vacuole via the CCV pathway.

AtVSR3 was expressed at low levels in mature embryos and was expressed ubiquitously in 7-d-old seedlings. However, beginning with the first true leaves, expression was limited to the hydathodes and guard cells until

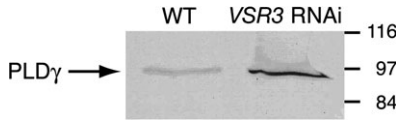

Fig. 7. PLDγ protein accumulation in *AtVSR3* RNAi and WT plants. Equal amounts of total protein extracts from leaves of WT and *AtVSR3* RNAi Line 3.1 were separated by SDS–PAGE, transferred to nitrocellulose membrane, and probed with antibodies raised against PLDγ.

flowering, at which point GUS activity was also detected in the anthers and carpels. The present RT-PCR results were, for the most part, consistent with those reported by Laval *et al*. (2003).

The localization pattern and RNAi analysis suggest a role for AtVSR3 in guard cell regulation and stomatal function

Because AtVSR3::GUS expression was localized to guard cells and hydathodes in 4-week-old plants, it was hypothesized that this sorting receptor was somehow involved in the regulation of water relations and, by extension, ABA signalling. ABA-induced stomatal opening involves a complex scheme of intermediates and both plasma membrane- and tonoplast-localized ion channels. ABA itself is responsible for an increase in cytosolic pH that triggers the activation of ion channels, and induces enzymes that are involved in the synthesis of signalling intermediates such as NO and reactive oxygen species (ROS). ABA biosynthesis occurs in response to stress from water deficits. ABA, in turn, causes an increase in cytoplasmic calcium ion concentration. Increased $[Ca^{2+}]_{cyt}$ activates anion channels that release anions from guard cells that lead to the depolarization of the guard cell plasma membrane. The change in membrane potential activates outward-rectifying K^+ channels and deactivates inward-rectifying K^+ channels, causing a net outflow of potassium ions and, subsequently, loss of guard cell turgor, leading to stomatal closing (Schroeder *et al*., 2001). It would not be unprecedented to determine that an endomembrane system component is involved in osmotic regulation. A number of studies have linked trafficking proteins such as NtSYR1 (Geelen *et al*., 2002), AtSYP61 (Zhu *et al*., 2002), and the ABC transporters AtMRP4 (Klein *et al*., 2004) and AtMRP5 (Klein *et al*., 2003) to guard cell regulation and function.

To test further the hypothesis that AtVSR3 may also be involved in stomatal regulation pathways, RNAi lines that exhibited either lower or no expression of the *AtVSR3* gene were created. The *AtVSR3* RNAi lines have no obvious morphological defects. Furthermore, the RNAi lines had comparable numbers of stomates as compared with the WT control line, although a larger proportion were opened based on a 2.5 μm cut-off (no ABA treatment). They also have a compacted lifecycle; *VSR3* RNAi plants bolt, set seed, and senesce earlier than WT control plants of comparable chronological age. More detailed analysis of one of the RNAi lines (Line 3.1) revealed additional phenotypes; these include less stomatal closure following treatment with ABA, and a mean leaf temperature 0.8 °C lower than that of wild-type (WT). *AtVSR3* Line 3.1 RNAi plants also feature constitutively higher levels of H_2O_2, NO, and PLDγ in guard cells.

The phytohormone ABA is known to play a role in the induction of senescence (Yang *et al*., 2001; Pourtau *et al*., 2004). Enhanced carbon remobilization and accelerated grain filling have been observed in wheat plants when subjected to water stress (Yang *et al*., 2003). These effects have been attributed to elevated ABA levels induced by drought conditions. The higher endogenous levels of ROS in the *AtVSR3* RNAi plants may indicate that the plants lacking AtVSR3 protein could be stressed to the point that they enter early senescence, which would correlate with the early flowering phenotype. The simplest explanation of the present results is that AtVSR3 operates upstream of NO and ROS production, in which case it may suppress endogenous levels of ROS and NO in the guard cells of wild-type plants.

It has been shown for a number of different plant species that levels of NO and H_2O_2 in guard cells rise in response to applied ABA, and that these increases promote decreases in stomatal apertures (Neill *et al*., 2003; Desikan *et al*., 2004). Furthermore, increases in endogenous levels of ABA induce synthesis of these two intermediate signalling molecules in plant cells. Pharmacological data indicate that MAP kinases are involved in both ABA- and H_2O_2-induced stomatal closing pathways. It is unclear at this point whether H_2O_2 and NO are also involved in stomatal opening, pathways that are distinct from those that control the closing of guard cells.

Proteomic analysis of WT and *VSR3* RNAi plants demonstrated that the RNAi plants display higher levels of PLDγ1. Phospholipases hydrolyse phospholipids to produce phosphatidic acid and free head group. Phosphatidic acid may act in signal transduction pathways, cytoskeletal rearrangements, membrane lipid degradation, and, significantly, vesicular trafficking (Zhang *et al*., 2005). The *Arabidopsis* genome contains 12 *PLD* genes, including three *PLDγ* genes that feature Ca^{2+}-dependent phospholipid-binding C2 domains (Zhang *et al*., 2005; Qin *et al*., 2006). Specific PLDs function in different plant stress pathways; PLDα1 has been shown to promote ROS production, which leads to stomatal closure, whereas PLDδ mediates other responses to ROS (Zhang *et al*., 2005). Less is known about the function(s) of PLDγ1. PLDγ has been localized to the plasma membrane, intracellular membranes, mitochondria, CCV, cytosol, and nucleus (Fan *et al*., 1999). *Arabidopsis* plants challenged with avirulent or virulent *Pseudomonas syringae* cultures show an enhanced and sustained elevation of PLDγ1 expression during incompatible reactions, suggesting that it might play a role during gene-to-gene interactions that lead to the hypersensitive response (Zabela *et al*., 2002). PLDγ also contains a putative amino-terminal myristoylation site that is not found in the α or β forms of the protein (Qin *et al*., 1997). The C2 and myristoylation domains of a number of proteins are involved in protein–membrane interactions, so it may be possible that these domains regulate the association of PLDγ with target membranes. Increased PLDγ1 was detected in *VSR3*

RNAi crude cellular extracts. Whether the loss of VSR3 protein results in cellular stresses that impact on the levels of PLDγ1 at the transcriptional level, or alters the relative amounts of soluble and membrane-bound protein, will be addressed in future experiments.

Defects in stomatal movement and lower leaf temperatures in the *VSR3* RNAi line may implicate a role for VSR3 in guard cell function; the accelerated life cycle phenotype most likely indicates that lack of VSR3 protein causes systemic stress in affected plants. What is not clear at this point is the mechanism by which VSR3 may regulate stomatal function. A recently published study has demonstrated that vacuolar fusion is necessary for guard cell expansion; it may be possible that VSR3 is necessary for this process (Gao *et al*., 2005). It will be necessary to determine the subcellular localization of VSR3 and to uncover the identities of proteins with which it may interact. In a recent publication it was shown that all seven AtVSRs are localized to multivesicular bodies in tobacco BY-2 cells (Miao *et al*., 2006); however, higher resolution data from non-heterologous experimental systems is still required. It will be of interest to determine whether other molecules involved in protein trafficking and guard cell regulation, such as SYP61 and PLDγ1, interact specifically with VSR3 or VSR3-containing vesicles. Studies of the vacuole proteome have already demonstrated that there is no appreciable VSR3 protein associated with that compartment, although it should be noted that this determination was made using protoplasts derived from whole rosette leaves (Carter *et al*., 2004). The most obvious mechanistic explanation is that plants lacking VSR3 protein fail to transport a particular cargo to the vacuole, thus altering the vacuole in such a manner as to either prevent vacuolar fusion or to impede ion flux to and from the vacuole. However, at this point, a novel regulatory role cannot be ruled out. Further experiments will help clarify the role that membrane trafficking plays in guard cell regulation.

Acknowledgements

We thank Dr Xuemin Wang, for providing antibodies raised against PLDγ1 and for useful comments, and Dr Glen Hicks, Dr Jan Zouhar, and other members of the Raikhel laboratory for helpful discussions. Ms Jocelyn Brimo co-ordinated submission of the manuscript and assisted in the preparation of the figures. NSF MCB-0296080 (NVR), an NSF Graduate Research Fellowship (ELA), and the Leverhume Trust (RD and SJN) funded this study.

References

Ahmed SU, Bar-Peled M, Raikhel NV. 1997. Cloning and subcellular location of an Arabidopsis receptor-like protein that shares common features with protein-sorting receptors of eukaryotic cells. *Plant Physiology* **114,** 325–336.

Ahmed SU, Rojo E, Kovaleva V, Venkataraman S, Dombrowski JE, Matsuoka K, Raikhel NV. 2000. The plant vacuolar sorting receptor AtELP is involved in transport of NH(2)-terminal propeptide-containing vacuolar proteins in *Arabidopsis thaliana*. *Journal of Cell Biology* **149,** 1335–1344.

Bednarek SY, Wilkins TA, Dombrowski JE, Raikhel NV. 1990. A carboxyl-terminal propeptide is necessary for proper sorting of barley lectin to vacuoles of tobacco. *The Plant Cell* **2,** 1145–1155.

Bonifacino JS, Dell'Angelica EC. 1999. Molecular bases for the recognition of tyrosine-based sorting signals. *Journal of Cell Biology* **145,** 923–926.

Carter C, Pan S, Zouhar J, Avila EL, Girke T, Raikhel NV. 2004. The vegetative vacuole proteome of *Arabidopsis thaliana* reveals predicted and unexpected proteins. *The Plant Cell* **16,** 3285–3303.

Clough SJ, Bent AF. 1998. Floral dip: a simplified method for *Agrobacterium*-mediated transformation of *Arabidopsis thaliana*. *The Plant Journal* **16,** 735–743.

Desikan R, Cheung MK, Bright J, Henson D, Hancock JT, Neill SJ. 2004. ABA, hydrogen peroxide and nitric oxide signalling in stomatal guard cells. *Journal of Experimental Botany* **55,** 205–212.

Desikan R, Griffiths R, Hancock J, Neill S. 2002. A new role for an old enzyme: nitrate reductase-mediated nitric oxide generation is required for abscisic acid-induced stomatal closure in *Arabidopsis thaliana*. *Proceedings of the National Academy of Sciences, USA* **99,** 16314–16318.

Fan L, Zheng SQ, Cui DC, Wang XM. 1999. Subcellular distribution and tissue expression of phospholipase D alpha, D beta, and D gamma in Arabidopsis. *Plant Physiology* **119,** 1371–1378.

Felsenstein J. 1997. An alternating least squares approach to inferring phylogenies from pairwise distances. *Systematic Biology* **46,** 101–111.

Gao XQ, Li CG, Wei PC, Zhang XY, Chen J, Wang XC. 2005. The dynamic changes of tonoplasts in guard cells are important for stomatal movement in *Vicia faba*. *Plant Physiology* **139,** 1207–1216.

Geelen D, Leyman B, Batoko H, Di Sansebastiano GP, Moore I, Blatt MR. 2002. The abscisic acid-related SNARE homolog NtSyr1 contributes to secretion and growth: evidence from competition with its cytosolic domain. *The Plant Cell* **14,** 387–406.

Happel N, Honing S, Neuhaus JM, Paris N, Robinson DG, Holstein SEH. 2004. Arabidopsis mu A-adaptin interacts with the tyrosine motif of the vacuolar sorting receptor VSR-PS1. *The Plant Journal* **37,** 678–693.

Hinz G, Colanesi S, Hillmer S, Rogers JC, Robinson DG. 2007. Localization of vacuolar transport receptors and cargo proteins in the Golgi apparatus of developing Arabidopsis embryos. *Traffic* **8,** 1452–1464.

Hohl I, Robinson DG, Chrispeels MJ, Hinz G. 1996. Transport of storage proteins to the vacuole is mediated by vesicles without a clathrin coat. *Journal of Cell Science* **109,** 2539–2550.

Holwerda BC, Padgett HS, Rogers JC. 1992. Proaleurain vacuolar targeting is mediated by short contiguous peptide interactions. *The Plant Cell* **4,** 307–318.

Kirsch T, Paris N, Butler JM, Beevers L, Rogers JC. 1994. Purification and initial characterization of a potential plant vacuolar targeting receptor. *Proceedings of the National Academy of Sciences,* USA **91,** 3403–3407.

Klein M, Geisler M, Suh SJ, *et al*. 2004. Disruption of AtMRP4, a guard cell plasma membrane ABCC-type ABC transporter,

leads to deregulation of stomatal opening and increased drought susceptibility. *The Plant Journal* **39,** 219–236.

Klein M, Perfus-Barbeoch L, Frelet A, Gaedeke N, Reinhardt D, Mueller-Roeber B, Martinoia E, Forestier C. 2003. The plant multidrug resistance ABC transporter AtMRP5 is involved in guard cell hormonal signalling and water use. *The Plant Journal* **33,** 119–129.

Laemmli UK. 1970. Cleavage of structural proteins during the assembly of the head of bacteriophage T4. *Nature* **227,** 680–685.

Laval V, Chabannes M, Carriere M, Canut H, Barre A, Rouge P, Pont-Lezica R, Galaud JP. 1999. A family of Arabidopsis plasma membrane receptors presenting animal beta-integrin domains. *Biochimica et Biophysica Acta – Protein Structure and Molecular Enzymology* **1435,** 61–70.

Laval V, Masclaux F, Serin A, Carriere M, Roldan C, Devic M, Pont-Lezica RF, Galaud JP. 2003. Seed germination is blocked in Arabidopsis putative vacuolar sorting receptor (atbp80) antisense transformants. *Journal of Experimental Botany* **54,** 213–221.

Li YB, Rogers SW, Tse YC, Lo SW, Sun SSM, Jauh GY, Jiang LW. 2002. BP-80 and homologs are concentrated on post-Golgi, probable lytic prevacuolar compartments. *Plant and Cell Physiology* **43,** 726–742.

Mahon P, Bateman A. 2000. The PA domain: a protease-associated domain. *Protein Science* **9,** 1930–1934.

Masclaux FG, Galaud JP, Pont-Lezica R. 2005. The riddle of the plant vacuolar sorting receptors. *Protoplasma* **226,** 103–108.

Matsuoka K, Bassham DC, Raikhel NV, Nakamura K. 1995. Different sensitivity to wortmannin of two vacuolar sorting signals indicates the presence of distinct sorting machineries in tobacco cells. *Journal of Cell Biology* **130,** 1307–1318.

Matsuoka K, Bednarek SY. 1998. Protein transport within the plant cell endomembrane system: an update. *Current Opinion in Plant Biology* **1,** 463–469.

Matsuoka K, Nakamura K. 1991. Propeptide of a precursor to a plant vacuolar protein required for vacuolar targeting. *Proceedings of the National Academy of Sciences, USA* **88,** 834–838.

Matsuoka K, Nakamura K. 1999. Large alkyl side-chains of isoleucine and leucine in the NPIRL region constitute the core of the vacuolar sorting determinant of sporamin precursor. *Plant Molecular Biology* **41,** 825–835.

McElroy D, Chamberlain DA, Moon E, Wilson KJ. 1995. Development of Gusa reporter gene constructs for cereal transformation – availability of plant transformation vectors from the Cambia Molecular-Genetic Resource Service. *Molecular Breeding* **1,** 27–37.

Melchers LS, Selabuurlage MB, Vloemans SA, Woloshuk CP, Vanroekel JSC, Pen J, Vandenelzen PJM, Cornelissen BJC. 1993. Extracellular targeting of the vacuolar tobacco proteins-Ap24, chitinase and beta-1,3-glucanase in transgenic plants. *Plant Molecular Biology* **21,** 583–593.

Merlot S, Mustilli AC, Genty B, North H, Lefebvre V, Sotta B, Vavasseur A, Giraudat J. 2002. Use of infrared thermal imaging to isolate Arabidopsis mutants defective in stomatal regulation. *The Plant Journal* **30,** 601–609.

Miao Y, Yan PK, Kim H, Hwang I, Jiang L. 2006. Localization of green fluorescent protein fusions with the seven Arabidopsis vacuolar sorting receptors to prevacuolar compartments in tobacco BY-2 Cells. *Plant Physiology* **142,** 945–962.

Miller EA, Lee MCS, Anderson MA. 1999. Identification and characterization of a prevacuolar compartment in stigmas of *Nicotiana alata*. *The Plant Cell* **11,** 1499–1508.

Neill SJ, Desikan R, Hancock JT. 2003. Nitric oxide signalling in plants. *New Phytologist* **159,** 11–35.

Neuhaus JM, Sticher L, Meins Jr F, Boller T. 1991. A short C-terminal sequence is necessary and sufficient for the targeting of chitinases to the plant vacuole. *Proceedings of the National Academy of Sciences, USA* **88,** 10362–10366.

Notredame C, Higgins DG, Heringa J. 2000. T-Coffee: a novel method for fast and accurate multiple sequence alignment. *Journal of Molecular Biology* **302,** 205–217.

Olbrich A, Hillmer S, Hinz G, Oliviusson P, Robinson DG. 2007. Newly formed vacuoles in root meristems of barley and pea seedlings have characteristics of both protein storage and lytic vacuoles. *Plant Physiology* **145,** 1383–1394.

Otegui MS, Herder R, Schulze J, Jung R, Staehelin LA. 2006. The proteolytic processing of seed storage proteins in arabidopsis embryo cells starts in the multivesicular bodies. *The Plant Cell* **18,** 2567–2581.

Pan S, Gu S, Bradbury EM, Chen X. 2003. Single peptide-based protein identification in human proteome through MALDI-TOF MS coupled with amino acids coded mass tagging. *Analytical Chemistry* **75,** 1316–1324.

Pandey S, Wang XQ, Coursol SA, Assmann SM. 2002. Preparation and applications of *Arabidopsis thaliana* guard cell protoplasts. *New Phytologist* **153,** 517–526.

Paris N, Stanley CM, Jones RL, Rogers JC. 1996. Plant cells contain two functionally distinct vacuolar compartments. *Cell* **85,** 563–572.

Pei ZM, Murata Y, Benning G, Thomine S, Klusener B, Allen GJ, Grill E, Schroeder JI. 2000. Calcium channels activated by hydrogen peroxide mediate abscisic acid signalling in guard cells. *Nature* **406,** 731–734.

Pourtau N, Mares M, Purdy S, Quentin N, Ruel A, Wingler A. 2004. Interactions of abscisic acid and sugar signalling in the regulation of leaf senescence. *Planta* **219,** 765–772.

Qin C, Li M, Qin WS, Bahn SC, Wang C, Wang XM. 2006. Expression and chracterization of Arabidopsis phospholipase D gamma 2. *Biochimica et Biophysica Acta* **1761,** 1450–1458.

Qin WS, Pappan K, Wang XM. 1997. Molecular heterogeneity of phospholipase D (PLD): cloning of PLD gamma and regulation of plant PLD gamma, -beta, and -alpha by polyphosphoinositides and calcium. *Journal of Biological Chemistry* **272,** 28267–28273.

Rojo E, Zouhar J, Carter C, Kovaleva V, Raikhel NV. 2003. A unique mechanism for protein processing and degradation in *Arabidopsis thaliana*. *Proceedings of the National Academy of Sciences, USA* **100,** 7389–7394.

Saalbach G, Kunze G, Christov V, Adler K, Muntz K. 1991. Vacuolar targeting in intracellular-transport of plant seed proteins in yeast. *Biological Chemistry Hoppe-Seyler* **372,** 740–740.

Sambrook J, Russell DW. 2001. *Molecular cloning: a laboratory manual*. Cold Spring Harbor, NY: Cold Spring Harbor Laboratory Press.

Sanderfoot AA, Ahmed SU, Marty-Mazars D, Rapoport I, Kirchhausen T, Marty F, Raikhel NV. 1998. A putative vacuolar cargo receptor partially colocalizes with AtPEP12p on a prevacuolar compartment in Arabidopsis roots. *Proceedings of the National Academy of Sciences, USA* **95,** 9920–9925.

Sanderfoot AA, Pilgrim M, Adam L, Raikhel NV. 2001. Disruption of individual members of Arabidopsis syntaxin gene families indicates each has essential functions. *The Plant Cell* **13,** 659–666.

Schroeder JI, Allen GJ, Hugouvieux V, Kwak JM, Waner D. 2001. Guard cell signal transduction. *Annual Reviews of Plant Physiology and Plant Molecular Biology* **52,** 627–658.

Shimada T, Fuji K, Tamura K, Kondo M, Nishimura M, Hara-Nishimura I. 2003. Vacuolar sorting receptor for seed storage

proteins in *Arabidopsis thaliana*. *Proceedings of the National Academy of Sciences, USA* **100,** 16095–16100.

Shimada T, Kuroyanagi M, Nishimura M, Hara-Nishimura I. 1997. A pumpkin 72-kDa membrane protein of precursor-accumulating vesicles has characteristics of a vacuolar sorting receptor. *Plant and Cell Physiology* **38,** 1414–1420.

Shimada T, Watanabe E, Tamura K, Hayashi Y, Nishimura M, Hara-Nishimura I. 2002. A vacuolar sorting receptor PV72 on the membrane of vesicles that accumulate precursors of seed storage proteins (PAC) vesicles. *Plant and Cell Physiology* **43,** 1086–1095.

Tague BW, Dickinson CD, Chrispeels MJ. 1990. A short domain of the plant vacuolar protein phytohemagglutinin targets invertase to the yeast vacuole. *The Plant Cell* **2,** 533–546.

Tsuru-Furuno A, Okamoto T, Minamikawa T. 2001. Isolation of a putative receptor for KDEL-tailed cysteine proteinase (SH-EP) from cotyledons of *Vigna mungo* seedlings. *Plant and Cell Physiology* **42,** 1062–1070.

Vitale A, Raikhel NV. 1999. What do proteins need to reach different vacuoles? *Trends in Plant Science* **4,** 149–155.

Watanabe E, Shimada T, Kuroyanagi M, Nishimura M, Hara-Nishimura I. 2002. Calcium-mediated association of a putative vacuolar sorting receptor PV72 with a propeptide of 2S albumin. *Journal of Biological Chemistry* **277,** 8708–8715.

Weigel D, Glazebrook J. 2002. *Arabidopsis: a laboratory manual*. Cold Spring Harbor, NY: Cold Spring Harbor Laboratory Press.

Yang JC, Zhang JH, Wang ZQ, Zhu QS, Liu LJ. 2003. Involvement of abscisic acid and cytokinins in the senescence and remobilization of carbon reserves in wheat subjected to water stress during grain filling. *Plant, Cell and Environment* **26,** 1621–1631.

Yang JC, Zhang JH, Wang ZQ, Zhu QS, Wang W. 2001. Hormonal changes in the grains of rice subjected to water stress during grain filling. *Plant, Physiology* **127,** 315–323.

Zabela MD, Fernandez-Delmond I, Niittyla T, Sanchez P, Grant M. 2002. Differential expression of genes encoding Arabidopsis phospholipases after challenge with virulent or avirulent *Pseudomonas* isolates. *Molecular Plant-Microbe Interactions* **15,** 808–816.

Zhang WH, Yu LJ, Zhang YY, Wang XM. 2005. Phospholipase D in the signaling networks of plant response to abscisic acid and reactive oxygen species. *Biochimica et Biophysica Acta – Molecular and Cell Biology of Lipids* **1736,** 1–9.

Zhu J, Gong Z, Zhang C, Song CP, Damsz B, Inan G, Koiwa H, Zhu JK, Hasegawa PM, Bressan RA. 2002. OSM1/SYP61: a syntaxin protein in Arabidopsis controls abscisic acid-mediated and non-abscisic acid-mediated responses to abiotic stress. *The Plant Cell* **14,** 3009–3028.